Journal of Food Engineering **35** (1998) 395–407
© 1998 Elsevier Science Limited. All rights reserved
Printed in Great Britain
PII: S0260-8774(98)00036-3
0260-8774/98 $19.00+0.00

Experimental and Theoretical Study of Model Food Freezing. Part II. Characterization and Modelling of the Ice Crystal Size

B. Woinet[a], J. Andrieu[a]*, M. Laurent[b] & S.G. Min[c]

[a]Laboratoire d'Automatique et de Genie des Procédés (LAGEP), UPRES A Q5007,
UCB-Lyon I-CPE bât. 308G, 43, bd du 11 Novembre 1918, 69622 Villeurbanne, France
[b]Centre de Thermique de Lyon (CETHIL), UPRES A Q5008, INSA-Lyon I, bât 404,
20 av. A. Einstein, 69621 Villeurbanne, France
[c]Laboratory of Food Engineering, Department of Livestock Technology,
College of Animal Husbandry, Kon-Kuk University, 93, Mojin-dong, Seongdong-gu, Seoul,
Korea

(Received 7 August 1997; accepted 17 February 1998)

ABSTRACT

Frozen gelatin gels were freeze-dried, then sliced, microphotographed and analyzed with image analysis software. A mean ice crystal size was determined at different locations inside the gel for many operating conditions and different gelatin concentrations with or without ionic solute (sodium chloride). It was observed that the mean ice crystal size grew proportionally with the distance from the cold plate. Ionic solute addition had a great influence on the mean ice crystal size. A model based on the principle of the supercooling resulting from the maximum concentration difference in the interdendritic zone was able to justify the experimental relationship and to interpret quantitatively these data.
© 1998 Elsevier Science Limited. All rights reserved

NOMENCLATURE

a_j	Thermal diffusivity of j zone (m2/s)
C_j	Concentration of j component (kmol/m^3)
d_p	Ice crystal size (m)
d_p^*	Mean ice crystal size (m)
D_j	Mass diffusion coefficient of j component (m^2/s)
G_j	Temperature gradient in the j zone (°C/m)

---

*To whom correspondence should be addressed.

k	Constant of the freezing front rate (m^2/s)
L	Dendritic spacing (m)
m	Slope of the water-solute liquidus curve (°C.m^3/kmol) or (°C)
p	Interdendritic half distance (m)
Q	Cumulative distribution
R	Axial freezing front rate (m/s)
s	Initial freezing front position (m)
t	Time (s)
T	Temperature (°C)
T_j	Temperature of j zone (°C)
T_{I}	Cooling temperature (°C)
T_{II}	Initial temperature (°C)
$T(C_j)$	Temperature in equilibrium with j concentration (°C)
T_{m}	Initial freezing temperature (°C)
y	Abscissa in the transverse direction (m)
z	Abscissa in the heat flux direction (m)

Greek symbols

$\Delta C_{a,j}$	Solute concentration difference in the j direction (kg/m^3)
ΔT_y	Supercooling in the interdendritic space relative to $\Delta C_{a,j}$ (°C)
ΔT_z	Temperature difference ahead of the front relative to $\Delta C_{a,z}$ (°C)
$\gamma = \rho_2/\rho_1$	Unfrozen and frozen zones density ratio

Subscripts

1	Frozen zone
2	Unfrozen zone
a	Solute (sodium chloride)

Mathematical expression

$$F[x] = \sqrt{\pi} \cdot x \cdot \exp(x^2) \cdot erfc(x)$$

INTRODUCTION

It is well known by food technologists that the freezing rate has a strong influence on the texture of frozen foods, mainly on ice crystal size distribution: low freezing rates lead to large ice crystal sizes and fast freezing rates give generally small ice crystal sizes. For natural cellular foodstuffs (fruits, vegetables) bigger ice crystals involve cellular wall destruction and organoleptic quality losses during the thawing step. In order to optimize industrial freezing chains on a scientific basis, the aim of this work was to characterize the ice crystal size of model frozen foods and, then, to establish a theoretical relationship between the crystal size, the characteristics of the material and the freezing operating conditions.

There is, however, very few published literature data on these topics, belonging to alloy solidification systems (Tiller & Rutter, 1956; Rohatgi & Adams, 1967b) or to food freezing systems (Bevilacqua *et al.*, 1979; Bomben & King, 1982; Miyawaki *et al.*, 1992).

The experiments reported here were carried out with gelatin gels, the thermophysical properties of which were extensively determined in the first part of this research program (Woinet *et al.*, 1998). Other unpublished data were obtained with commercial foodstuffs (ice cream, yoghourt,...) by the same methodology (Woinet, 1997).

ICE CRYSTAL SIZE DETERMINATION

Crystallization phenomenon

Gelatin gels were frozen in a freezing apparatus which ensured a unidirectional heat flux through the sample in contact with a cooled copper plate (Woinet, 1997). The crystallization phenomenon inside the sample took place in different steps: during the first step very few nuclei appeared suddenly on the surface of the copper plate. Then, during the second step, surface crystallization from these nuclei developed rapidly all over the copper plate area. Finally, during the third step a plane freezing front, parallel to the copper plate surface, migrated into the sample away from this plate, with a freezing front rate noted *R*. A schematic view of the frozen zone is presented below on Fig. 1:

— A slice parallel to the heat flux showed a cellular morphology of the ice crystals: this structure was characterized by ice fingers parallel to the heat flux and separated from each others by concentrated dry matter. The size of these fingers increased with the distance from the cooling plate at the expense of others which stopped to grow.

— A slice perpendicular to the heat flux showed sections of ovoid shape.

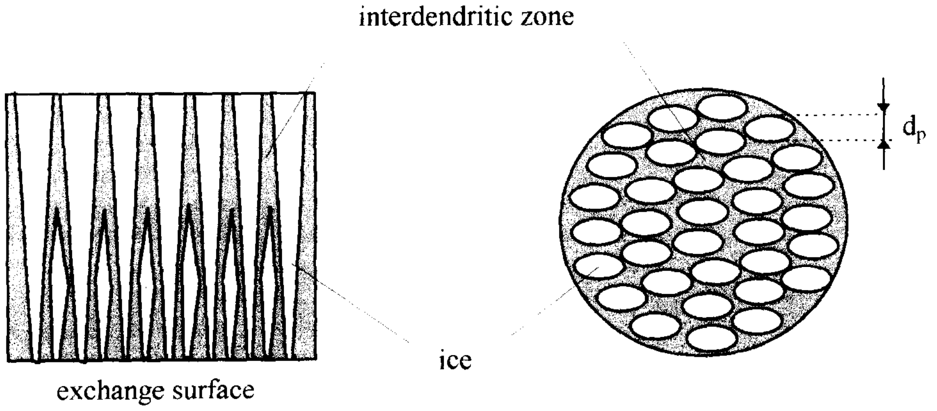

Cut parallel to the heat flux

Cut perpendicular to the heat flux

Fig. 1. Schematic structure of the model gel in the frozen state.

As was adopted by previous authors, it was assumed for a morphological reason that the crystal size, noted d_p, which will be measured, corresponded to the width or to the minor diameter of the ovoid section (Bevilacqua *et al.*, 1979; Miyawaki *et al.*, 1992). It is important to note here that generally the water all through the sample crystallized from very few nuclei, or even just from a single one. So, in this last case we could consider that the frozen sample was constituted by one single crystal; thus, it could seem incorrect to speak about crystal sizes. This d_p value would be defined in fact as an ice segregation degree within its interdendritic zone. Furthermore, that could probably mean that nucleation kinetics had no significant influence on the ice crystal size d_p.

Methodology of ice crystal size characterization

When the sample was completely frozen, the main problem was to set up an ice crystal size characterization methodology. Bomben and King (1982) observed the ice crystals directly on a scanning electronic microscope. This solution was rejected because of its high cost.

Firstly, the glutaraldehyde fixation method was chosen (Miyawaki *et al.*, 1992). This method consisted in immersing the frozen sample into a cold 4% glutaraldehyde water solution. This dialdehyde migrated into the thawing sample and created covalent bridges between the gelatin chains. So, the concentrated dry matter structure was maintained and then could be observed at ambient temperature. Nevertheless, this method proved to be suited only for products with high protein concentrations and was affected by several technical problems.

Then, the freeze-drying method, which is commonly used by authors working on freeze-drying studies (Kochs *et al.*, 1993; Sagara & Ichiba, 1994), was chosen. When the freezing step was achieved, a vacuum chamber was put all around the freezing cell. A vacuum pump and an ice trap with a cooling device maintained at −50°C were used to recover the condensed water vapor. The other cooling device was used to bring heat to the sample to promote the sublimation (Woinet *et al.*, 1998). At the beginning, its temperature had to be just below the vitreous transition temperature of the sample to avoid ice melting and collapse effects. Then, at the end of the drying process, this temperature was progressively increased to 40°C, to eliminate most of the adsorbed water, and to be sure to recover a vitreous state dry matter. After two or three days, the sample freeze-drying was finished. A dry sample weighing was used to check that the sample contained a low percentage of water, namely below 10% (dry basis). So, the structure of the concentrated dry matter as in its frozen state was recovered, if it was assumed that the pores replaced ice crystals. This freeze-drying method was well suited to low concentrated gelatin gels, thus limiting its application field, but it could be applied to others types of model foods or even foodstuffs (Woinet, 1997).

Then, the freeze-dried sample was cut in thin slices parallel to the copper plate with a thin cutter. Each slice was photographed with a stereomicroscope (Carl Zeiss, SV-6). The ice crystals, or in fact the pores, were measured by the means of the semi-automatic image analysis software (PPM, Arndt and Baumgartel GmbH). It consisted on projecting each slide on a graphic tablet driven by the computer; a graphic mouse allowed the identification of each crystal with four points, the small and the large diameters. Then, the software measured the size d_p, according to a corresponding previous calibration. For each slide, approximately 100 up to 500 crystals were measured, so giving the crystal size distribution. These distributions were fitted with the Rosin, Rammler, Spering and Bennet (R.R.S.B.) distribution function, which yielded the mean size d_p^*. This mean size was equal to the size corresponding to the value 0.632 of the cumulative distribution.

RESULTS AND DISCUSSION

Examples on Fig. 2 show the crystal size distribution at five positions for a typical experiment, and the corresponding R.R.S.B. distribution profiles. Two mean observations could be made for all the experiments realized:

- the mean size d_p^* increased with the distance from the copper plate;
- the width of the distribution increases with the distance from the copper plate.

In the case of gelatin gels without salt (Woinet *et al.*, 1997; Woinet *et al.*, 1996), the main following observations could be made (Fig. 3). Firstly, there is approximately a linear relationship between the mean ice crystal size d_p^* and the axial position z. For the same gel composition (2% gelatin) and the same initial temperature T_{ii}, the lower the cooling temperature T_l, the lower the mean size at a given position, and the smaller the 'thickening' coefficient corresponding to the slope of the linear regression line. In the case of the freezing by liquid nitrogen ($T_l = -185°C$), the mean size was practically the same all along the axial position z, so the frozen structure was more homogeneous than with a higher cooling temperature. An experiment had been made with a higher initial temperature (19.7°C). This different value involved a different gel behaviour not only because of the modified heat transfer, but also because of a different microscopic structure of the gelatin network. At room temperature, the ripening was slower than at a lower temperature, and so, the junction areas were less numerous but longer, which gave different gel rheological characteristics. As previously indicated (Woinet *et al.*, 1998), the initial

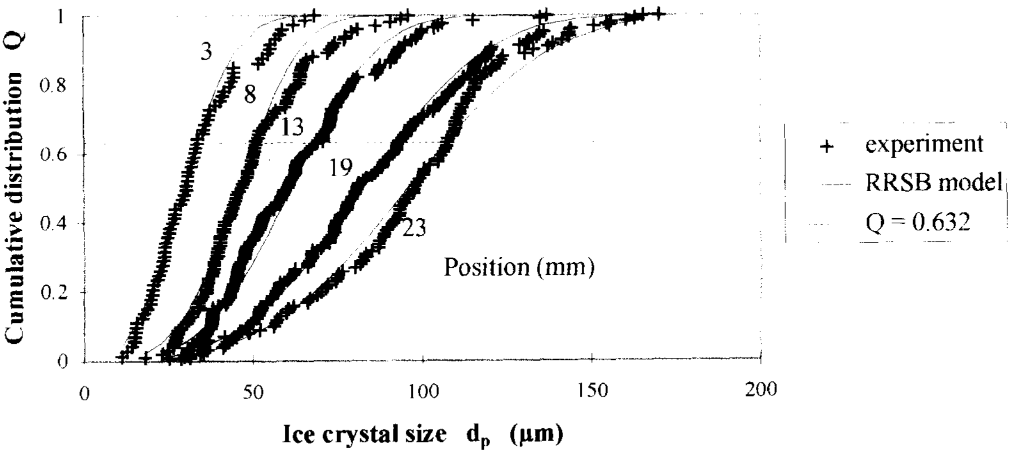

Fig. 2. Crystal size distribution for five axial positions; fine black curves: R.R.S.B. function.

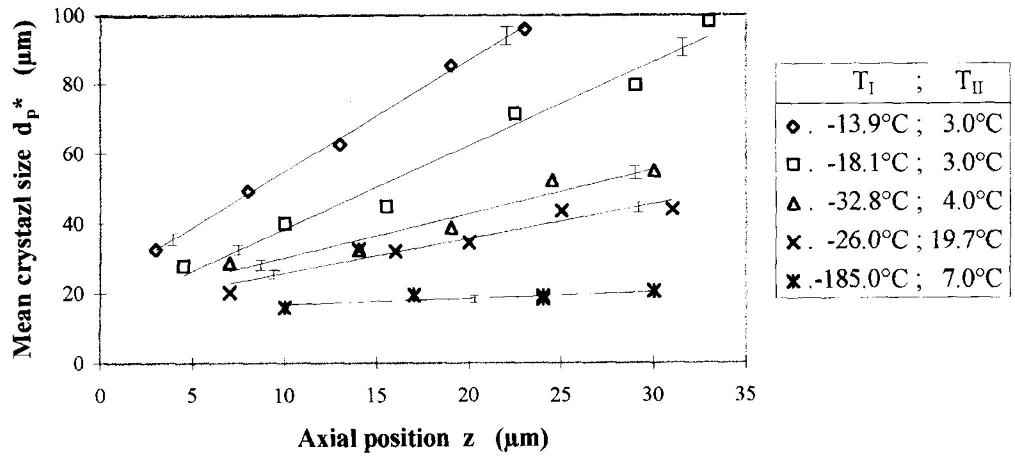

Fig. 3. 2% gelatin gel frozen at several cooling temperatures T_I.

temperature had an important influence on T_m values due to this phenomenon. So, despite the control of the ripening time of the gel before freezing, it was not possible to study the influence of the initial gel temperature on the ice crystal size because of the influence of the mechanical properties. Concerning the composition, it was not possible to study extensively the influence of the gelatin concentration, because experimentally, it was pretty difficult to freeze-dry gelatin gels more concentrated than 2%.

In the case of gelatin gels with salt we observed also a linear relationship between d_p* and z (Fig. 4), with an intercept which is notably different from zero. We do not

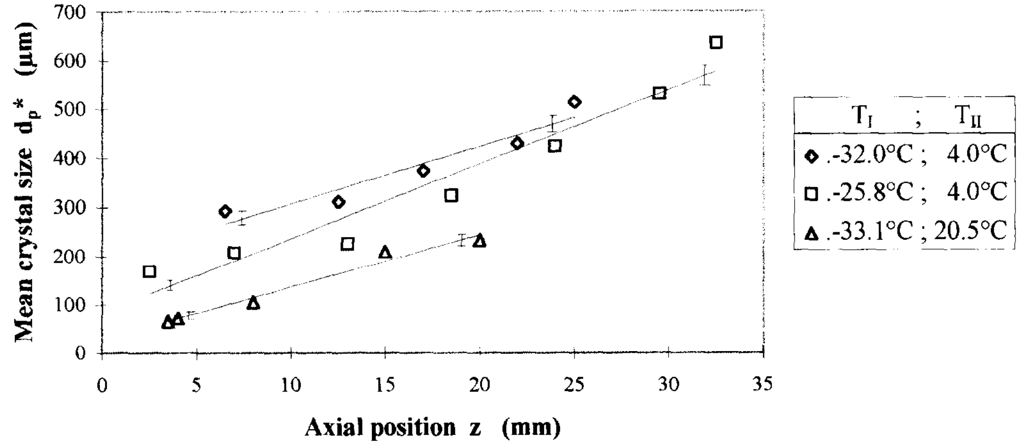

Fig. 4. Crystal size evolution in 2% gelatin gel with 1% NaClfor several operating conditions T_I and T_{II}.

have, at the present time, any satisfactory explanation of this fact. The comparison of the ordinates of Figs 3 and 4 showed the great difference between the mean crystal sizes in gelatin gels without salt, between 20 and 100 μm, and in gelatin gels with salt, between 100 and 600 μm under the same range of conditions. The salt addition lead to a considerable increase of the crystal sizes.

MODELLING

Supercooling resulting from the maximum concentration difference

The model was based on the principle of the supercooling resulting of the maximum concentration difference in the interdendritic zone (Rohatgi & Adams, 1967a,b). In a general case, the model food system was considered as a mixture of water, solute and gel. It was assumed that the gelatin mass diffusion inside the gel was not the limiting step and that the gel network inhibited any convection effect. The system had an equilibrium diagram with a straight liquidus line of slope $-m$. The water was assumed to crystallize in a temperature interval and with a cellular morphology, as shown in Fig. 5. The cellular tips corresponded to the initial freezing front ($z = s$).

Consider two adjacent crystals, the tips of which were separated by the dendritic spacing named L, and were schematized by vertical and plane plates. These plates were getting thicker during the cooling, and so rejected the solute into the center of the interdendritic region in the y-direction. This phenomenon created solute concentration gradients inside this interdendritic zone. Temperature gradients in this direction were neglected because of the very slow crystallization process, and because the heat diffusivity value was very high compared to the mass diffusivity

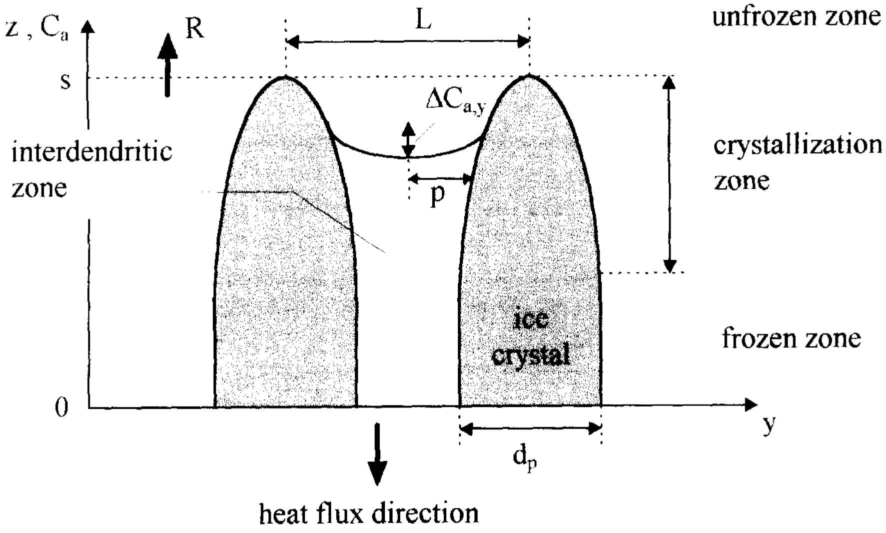

Fig. 5. Aqueous system freezing with a cellular morphology.

value. Thus, if we considered that the solid–liquid phase change at the interface took place at the thermodynamic equilibrium, all the interdendritic zone was in a metastable state due to a lower solute concentration than at the interface. So, a situation of supercooling existed. The maximum solute concentration difference $\Delta c_{a,y}$ between the interface and the center of the interdendritic zone involved a maximum supercooling Δt_y, given by the linear thermodynamic relationship:

$$\Delta T_y = m \cdot \Delta C_{a,y} \tag{1}$$

From the second Fick's law Rohatgi and Adams (1967a,b) showed that ΔT_y could be expressed as follows:

$$\Delta T_y = -\frac{p^2}{2D_a}\frac{dT}{dt} \tag{2}$$

where p is the half distance between two adjacent ice crystal plates and D_a is the solute mass diffusion coefficient. To adapt this equation at the position of the initial freezing front, that expression eqn (2) could be written:

$$\Delta T_y = -\frac{L^2}{8D_a}\left.\frac{dT}{dt}\right|_{z=s} \tag{3}$$

ΔT_y and D_a being constant, the dendritic spacing L appeared to be directly related to the cooling rate. Besides, this cooling rate was equal to the product of the temperature gradient G_1 in the frozen zone at the position s^- by the axial freezing front rate R. Then a direct relationship was obtained between the dendritic spacing L and the product $G_1^{-0.5}R^{-0.5}$ (Bomben & King, 1982). Furthermore, it had been shown experimentally that the thermal gradient could be considered constant all through the crystallization and the frozen zones. Thus, taking into account the variation of the freezing front position s = f(t) (Woinet *et al.*, 1998), G_1 was given by this simple expression:

$$G_1 = \frac{T_m - T_l}{s-0} = \frac{T_m - T_l}{\sqrt{k}\sqrt{t}} \tag{4}$$

R was obtained by derivation of s as a function of time:

$$R = \frac{ds}{dt} = \frac{1}{2}\frac{\sqrt{k}}{\sqrt{t}} \tag{5}$$

In the case of a low amount of dry matter, the final size of the crystal d_p was practically equal to the dendritic spacing L. Thus, by combining eqns (3)–(5) the following equation was obtained:

$$d_p \approx L = s \cdot \sqrt{\frac{16 \cdot \Delta T_y \cdot D_a}{k \cdot (T_m - T_l)}} = s \cdot Constant \tag{6}$$

The term under the square root could be considered constant during a freezing experiment. Thus, a direct and linear relationship between the crystal size d_p and the position *s* was obtained, as observed experimentally. The intercept, which is zero for eqn (6), was different from zero experimentally. This was probably due to non perfect Neumann conditions during the experiments. It was also observed that the data obtained with gels without salt agreed with the model, even if this model assumed a progressive crystallization in a temperature interval, which is not the case for this system.

Model validation

To express the supercooling ΔT_y as a function of known parameters, it was assumed that the concentration differences between the cellular tip and the center of the interdendritic zone, in the *y*-direction, and between the tip and the bulk unfrozen zone, in the *z*-direction, were equal. This hypothesis implied the equality between the supercooling ΔT_y and the temperature difference ΔT_z proportional to $\Delta C_{a,z}$:

$$\Delta C_{a,y} = \Delta C_{a,z} \Leftrightarrow \Delta T_y = \Delta T_z \tag{7}$$

The main problem was to determine the concentration difference which existed ahead of the freezing front, that is to say, to evaluate the solute accumulation at the level of the crystal tips. Körber (1988) and Kourosh *et al.* (1990) showed experimentally that in the case of solidification of alloys and of aqueous solutions this concentration difference was very low or even negligible. Thus, it was assumed that $\Delta C_{a,z}$ had the minimal possible value so that we were in the limit between the plane and the cellular morphologies. This principle was commonly named 'the condition of marginal equilibrium' (Fig. 6) (Worster, 1986). The limit between both morphologies could be described by Rutter and Chamlers instability criteria (Eustathopoulos *et al.*, 1988): in these conditions the temperature gradient and the temperature gradient in equilibrium with the concentration gradient, just ahead of the freezing front, were equal:

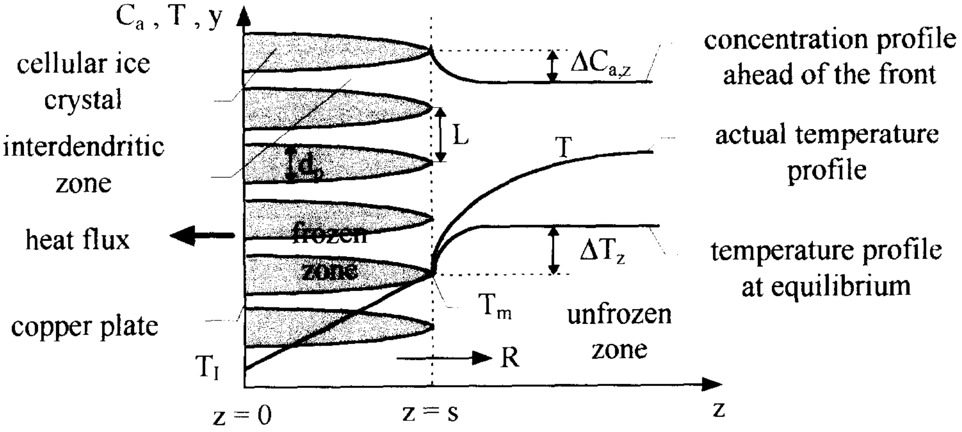

Fig. 6. Rutter and Chalmers' instability criteria.

$$\left.\frac{\partial T_2}{\partial z}\right|_{s'} = \left.\frac{\partial T(C_a)}{\partial z}\right|_{s'} = -m\left.\frac{\partial C_a}{\partial z}\right|_{s'} \tag{8}$$

The combination of eqn (8) with the heat transfer presented in the previous paper (Woinet *et al.*, 1998) lead to the following ΔT_z expression:

$$\Delta T_y = (T_{II} - T_m)\cdot\frac{D_a\cdot F[\sqrt{k}/(2\gamma\sqrt{D_a})]}{a_2\cdot F[\sqrt{k}/(2\gamma\sqrt{a_2})]} \tag{9}$$

and to the final expression relating d_p and the axial position s:

$$d_p = s\cdot\sqrt{\frac{16\cdot D_a^2}{k\cdot a_2}\,\frac{T_{II}-T_m}{T_m-T_I}\cdot\frac{F[\sqrt{k}/(2\gamma\sqrt{D_a})]}{\cdot F[\sqrt{k}/(2\gamma\sqrt{a_2})]}} \tag{10}$$

A purely theoretical study of this expression eqn (10) is presented on Fig. 7. The d_p/s ratio value, equivalent to the 'thickening' coefficient, was calculated as a function of the freezing operating conditions for a given composition. It was observed that this ratio is very small for low cooling temperatures and increased regularly with higher T_I values. So, the lower the cooling temperature, the weaker the size increasing versus axial position, and the smaller the ice crystal size. Furthermore, the higher the initial temperature, the greater the ratio value. This ratio sensitivity was very important when T_I and T_{II} are close to T_m temperature and decreased otherwise. The conclusions which could be made with this model justified the main empirical rules, i.e. that the freezing of a product, initially maintained at a temperature close to its freezing temperature, with a low cooling temperature gave the best quality. Contrary to other published models (Miyawaki *et al.*, 1992), this more advanced modelling took into account the influence of the gel initial temperature.

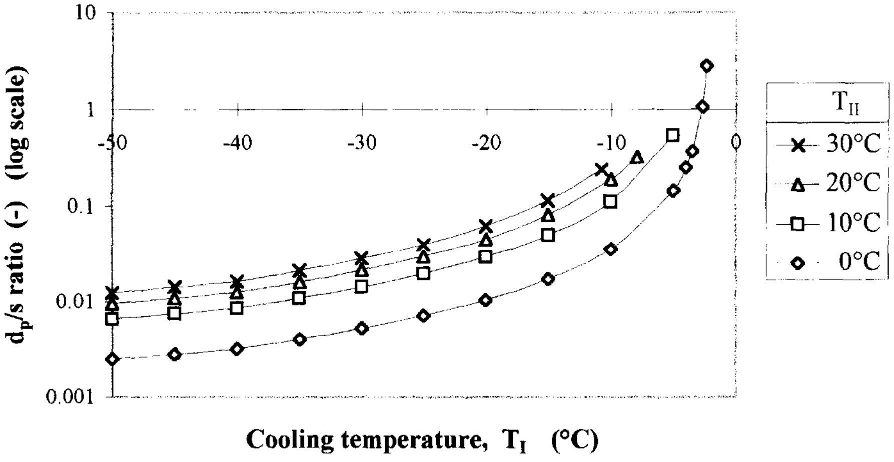

Fig. 7. dp/s ratio value as function of T_I and T_{II} for a given composition.

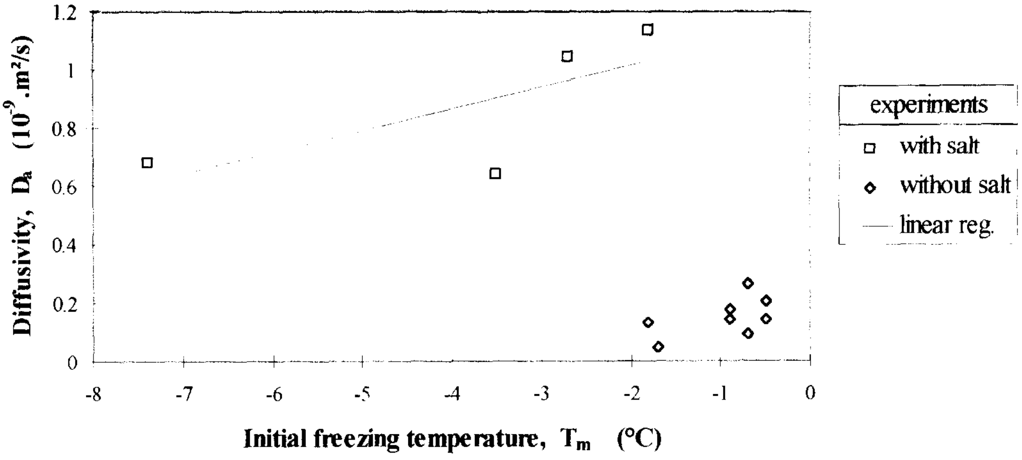

Fig. 8. Diffusion coefficient estimated values.

The model validation was achieved by estimating the diffusion coefficient values from the data obtained in the freezing experiments (temperatures, constant of the freezing front rate, thermophysical properties) (Woinet *et al.*, 1997). The D_a values are plotted on Fig. 8 as a function of T_m, because, as shown by eqn (3), this elementary process takes place at the initial freezing front.

Concerning the experiments with salt, the results were in a range close to values given by the literature: 1.29×10^{-9} m²/s (O'Callaghan *et al.*, 1980) or 0.78×10^{-9} m²/s (Wollhöver *et al.*, 1985). Furthermore, these values seemed to increase regularly with T_m, which was in agreement with the classical literature equations for diffusivity.

Concerning the experiments without salt, all results were gathered together around a mean value of approximately 0.2×10^{-9} m²/s, but it was difficult to give a physical interpretation of this result, principally because the condition of marginal equilibrium was normally not adapted to gelatin gels without salt.

CONCLUSION

Freezing experiments on gelatin gels with or without sodium chloride showed that the ice crystals adopted a cellular morphology. With heat transfer close to Neumann conditions, ice crystals increased proportionally with the distance from the cooling plate, the 'thickening' coefficient depending on composition and on freezing operating conditions. The salt addition lead to a considerable increase in the crystal size. An analytical relationship, based on the principle of the supercooling resulting from the maximum concentration difference in the interdendritic zone, was able to interpret the experimental results. With the hypothesis of the condition of marginal equilibrium, the final model was established and confirmed the main empirical rules concerning the influence of the initial temperature and of the cooling temperature on mean crystal size, i.e. on frozen food texture. Furthermore, this model was validated by comparing the solute mass diffusivity values estimated from the model and found in the literature. This new model, contrary to previous models, took into account the influence of the initial food temperature. Besides, as shown by unpublished data, it proved to be also suited for interpreting experimental data with commercial foodstuffs (yoghourt, ice cream,...).

ACKNOWLEDGEMENTS

The authors are grateful to MENESR and to Société AIR LIQUIDE (Centre de Recherche Claude Delorme) for their financial and technical assistance during this work.

REFERENCES

Bevilacqua, A., Zaritzky, N.E. & Calvelo, A. (1979). Histological measurements in frozen beef. *J. Food Technol.*, **14**, 237–251.

Bomben, J.L. & King, C.J. (1982). Heat and mass transport in the freezing of apple tissue. *J. Food Technol.*, **17**, 615–632.

Eustathopoulos, N., Camel, D. & Favier, J.J. (1988). La solidification à l'échelle de l'interface, 133–168. Dans Solidification des Alliages-du Procédé à la Microstructure, Ecole d'été Carry-le-Rouet, F. Durand, Les Editions de Physique.

Kochs, M., Körber, C., Heschel, I. & Nunner, B. (1993). The influence of the freezing process on vapour transport during sublimation in vacuum freeze-drying of macroscopic samples. *Int. J. Heat Mass Trans.*, **36**, 1727–1738.

Körber, Ch. (1988). Phenomena at the advancing ice–liquid interface: solutes, particles and biological cells. *Q. Rev. Biophys.*, **21**(2), 229–298.

Kourosh, S., Diller, K.R. & Crawford, M.E. (1990). Microscopic study of coupled heat and mass transport during unidirectional solidification of binary solutions—II. Mass transfer analysis. *Int. J. Heat Mass Trans.*, **33**(1), 39–53.

Miyawaki, O., Abe, T. & Yano, T. (1992). Freezing and ice structure formed in protein gels. *Biosci. Biotechnol. Biochem.*, **56**(6), 953–957.

O'Callaghan, M.G., Cravalho, E.G. & Huggins, C.E. (1980). Instability of the planar freeze front during solidification of an aqueous binary solution. *J. Heat Trans.*, **102**, 673–677.

Rohatgi, K. & Adams, M. (1967). Effect of freezing rates on dendritic solidification of ice from aqueous solutions. *Trans. Metallurgical Soc. AIME*, **239**, 1729–1736.

Rohatgi, K. & Adams, M. (1967). Dendritic solidification of aluminum-copper alloys. *Trans. Metallurgical Soc. AIME*, **239**, 1737–1746.

Sagara, Y. & Ichiba, J.I. (1994). Measurement of transport properties for the dried layer of coffee solution undergoing freeze-drying. *Drying Technol.*, **12**(5), 1081–1103.

Tiller, W.A. & Rutter, J.W. (1956). The effect of growth condition upon the solidification of a binary alloy. *Can. J. Phys.*, **34**, 96–121.

Woinet, B. (1997). Etude expérimentale et théorique de la cristallisation de l'eau dans les gels alimentaires congelés. Thèse de Doctorat, Lyon I.

Woinet, B., Andrieu, J., Laurent, M. & Min, S.G. (1996). Ice crystal size analysis in frozen model food gels. 5th World Congress of Chemical Engineering, San Diego, USA, 14–18 July, Vol. II, pp. 175–180.

Woinet, B., Andrieu, J. & Laurent, M. (1997). Theoretical and experimental study of mean ice crystal size in model frozen foods. 7th International Congress on Engineering and Food, Brighton, UK, 13–17 April, Part I, A5–A8.

Woinet, B., Andrieu, J. & Laurent, M. (1998). Experimental and theoretical study of model food freezing: Part I. Heat transfer modelling. *J. Food Engng*, **35**, 381–393.

Wollhöver, K., Körber, Ch., Scheiwe, M.W. & Hartmann, U. (1985). Unidirectional freezing of binary aqueous solutions: an analysis of transient diffusion of heat and mass. *Int. J. Heat Mass Trans.*, **28**(4), 761–769.

Worster, M.G. (1986). Solidification of an alloy from a cooled boundary. *J. Fluid Mech.*, **167**, 481–501.